# A global test of Allen's rule in rodents

Bader Alhajeri, Yoan Fourcade, Nathan Upham, Hasan Alhaddad

1    RUNNING HEAD: ALLEN'S RULE IN RODENTS

2

3    A GLOBAL TEST OF ALLEN'S RULE IN RODENTS

4

5    BADER H. ALHAJERI[1,†,*], YOAN FOURCADE[2,†], NATHAN S. UPHAM[3,4], HASAN

6    ALHADDAD[1],

7

8    [1]*Department of Biological Sciences, Kuwait University, Safat, 13060, Kuwait*

9    [2]*Sorbonne Université, UPEC, CNRS, IRD, INRAE, Institut d'écologie et des sciences de*

10   *l'environnement, IEES, F-75005 Paris, France*

11   [3]*Department of Ecology and Evolutionary Biology, Yale University, New Haven, CT, 06511,*

12   *USA*

13   [4]*School of Life Sciences, Arizona State University, Tempe, AZ, 85287, USA*

14

15   [†]BHA and YF contributed equally to this work and should be considered as co-first author.

16   *Corresponding author*: Bader H. Alhajeri (bader.alhajeri@ku.edu.kw)

17

30

## AUTHOR CONTRIBUTIONS

BHA conceived and designed the study and wrote the first draft of the manuscript. BHA, YF, NSU, and HA collected the data. BHA, YF, and NSU ran preliminary analyses. YF ran all the final analyses and produced the figures. BHA and YF wrote the final version of the manuscript with input from NSU and HA. All authors read and approved the final manuscript.

36

## BIOSKETCH

**BADER H. ALHAJERI** is an Associate Professor of Zoology in the Department of Biological Sciences at Kuwait University. He is interested generally in mammalian evolutionary ecology, and particularly the macroecological causes of morphological variation among species, at very broad spatial and taxonomic scales. Most of his research uses rodents as the study system. More information can be found on his website: https://sites.google.com/view/alhajeri.

**YOAN FOURCADE** is an Assistant Professor at Université Paris Est Créteil and in the Institute of Ecology and Environmental Sciences of Paris. He is broadly interested in conservation biology and spatial ecology. His current research topics deal with the interaction between local and macroecological processes in the context of climate change.

1

2    DR. BADER  H ALHAJERI  (Orcid ID : 0000-0002-4071-0301)

3    DR. YOAN   FOURCADE  (Orcid ID : 0000-0003-3820-946X)

4    DR. NATHAN   UPHAM  (Orcid ID : 0000-0001-5412-9342)

5

6

8

9

10    A GLOBAL TEST  OF ALLEN'S  RULE  IN RODENTS

11

12    **RUNNING TITLE:** ALLEN'S  RULE  IN RODENTS

13

**Abstract**

18    **Aim:** We test whether  geographic  variation  in length  of rodent species' appendages  follows

19    predictions  of Allen's  rule—a  positive  relationship  between  appendage  length  and temperature—

20    at a broad taxonomic  scale (order Rodentia).  We also test if the applicability  of this rule varies

21    based on the unit  of analysis  (species or assemblage),  examined  appendage  (tail, hind  foot,  ear),

22    body size, occupied  habitat,  geographic  range size, life mode,  and saltation  ability.

23    **Location:** Worldwide.

24    **Time period:** Current.

25    **Major taxa studied:** Rodents  (order Rodentia).

26    **Methods:** We assembled  data on morphology,  ecology,  and phylogeny  for up to 2,212 rodent

27    species—representing  ~86% of all the described  rodent species and ~95% of the described

28    genera. We tested  the predicted  Allen's  rule associations  among  size-corrected  appendage

29    lengths  and both latitude  and climatic  variables  (temperature  and precipitation).  We applied  a

30    cross-species  approach based on phylogenetic  regressions  and a cross-assemblage  approach

31    based on spatial regressions  in equal-area  1.5-degree  grid cells.

32 **Results:** Support for Allen's rule was greatest for the tail and was stronger across assemblages

33 than across species. We detected a negative relationship between tail length and (absolute)

34 latitude, which was accounted for by a positive association between tail length and temperature

35 of the coldest month. This association was greatest in desert species. In addition, we observed a

36 negative relationship between ear length and precipitation.

37 **Main conclusions:** In rodents, Allen's rule is confirmed only for tails, and this association seems

38 to be driven by adaptation to the cold, rather than warm temperatures. Habitat type seems to

39 influence conformity to this rule. Conformity to Allen's rule is likely the result of complex

40 evolutionary trade-offs between temperature regulation and other essential species' traits.

41

## 1 | INTRODUCTION

46 Allen's (1877) rule posits that the appendages (e.g., limbs, ears, tail, snout) of endotherms tend to

47 be longer and thinner in warmer environments. This rule is among the most studied

48 biogeographic patterns, perhaps second only to Bergmann's (1847) rule, which also makes a

49 prediction about the adaptive response of endothermic animals to climate. These rules are

50 related, and both are commonly interpreted as reoccurring geographic patterns in morphology

51 shaped by adaptation to climate. More specifically, the modification of surface-area-to-volume

52 ratio aids thermoregulation—its decrease in cold environments reduces heat loss and its increase

53 in warm environments facilitates heat dissipation (Mayr, 1956).

54     Allen's rule has been examined in various endotherms, including birds (e.g., Nudds &

55 Oswald, 2007; Symonds & Tattersall, 2010; McCollin et al., 2015) and mammals (e.g.,

56 lagomorphs: Griffing, 1974; Stevenson, 1986; primates: Fooden & Albrecht, 1999; Tilkens et al.,

57 2007; and rodents: Lindsay, 1987; Bidau et al., 2011; Alhajeri, 2016); it has also been examined

58 in ectotherms (e.g., Ray, 1960). So far, most mammal studies of Allen's rule were conducted at

59 the intraspecific level, while cross-species analyses are often restricted to a few species (often

60 within a taxonomically restricted group). However, recent mammal studies have explored the

61 applicability of this rule to broader taxonomic levels (e.g., Gohli & Voje, 2016; Alroy, 2019),

62 following up on earlier large-scale cross-species bird studies (e.g., Nudds & Oswald, 2007;

63  Symonds & Tattersall, 2010). Furthermore, cross-assemblage investigations of Allen's rule are

64  rare, if they exist at all, even though this approach is commonly used to study other

65  biogeographic trends (e.g., Blackburn & Hawkins, 2004; Olalla-Tárraga et al., 2010; Maestri et

66  al., 2016; Alhajeri et al., 2019). The role of ecological and geographic factors in conformity to

67  this rule is also an understudied topic. Recently, using a sample of 360 New World small

68  mammal species (marsupials, lipotyphlans, rodents), Alroy (2019) found evidence for longer

69  tails in tropical habitats (e.g., rainforests).

70      Here, we assemble an extensive dataset to test the predictions of Allen's rule globally in

71  Rodentia. Rodents are an outstanding system to study morphological responses to climate at the

72  interspecific level, especially since they comprise >2,000 extant recognized species (Mammal

73  Diversity Database, 2019) (leading to increased statistical power), have near-global geographic

74  distributions (IUCN, 2017) (encountering diverse climates), and vary greatly in body size

75  (Nowak, 1999) (facilitating the study of morphological covariation with climate). We aimed to

76  test whether rodents' appendage lengths (tail, hind foot, ear) vary consistently over geography

77  and climate, and whether Allen's rule can be similarly applied across rodent species as to spatial

78  assemblages of those species. We predict that phenotypes coherent with Allen's rule should be

79  more common in species with smaller geographic ranges because they are subject to a narrower

80  range of environmental conditions in which to adapt (see Alhajeri & Fourcade, 2019; Serrat et

81  al., 2008). We also predict a stronger appendage length – temperature association in smaller-

82  sized species—this is because in mammals, the relative effect of size modification on

83  thermoregulation (through changes in the surface-area to volume ratio) is greater in smaller

84  species, while in larger species, pelage modification plays a larger role in temperature control

85  (see Ashton et al., 2000; Alhajeri & Steppan, 2016; and references therein). Furthermore, based

86  on the results of Alhajeri (2016) and Alroy (2019), we expect Allen's rule to manifest most

87  strongly in rodent tails (compared to the hind foot and the ear), at tropical latitudes, and

88  specifically in deserts. The novelty of the present study stems from the near comprehensive (and

89  global) sampling of rodent species, the tests of influence of ecological factors on conformity to

90  this rule, and the comparison of cross-species vs. cross-assemblage analyses. The broad

91  taxonomic scale employed ensures that most of the covariation between appendage size and

92  temperature is a consequence of evolutionary adaptation via genetic selection (the mechanism

93  implied by most studies of Allen's and Bergmann's rules), rather than phenotypic plasticity.

94

## 2 | METHODS

### 2.1 | Morphometric data collection

We first compiled a list of all rodent species with range maps available in the International Union

for Conservation of Nature (IUCN, 2017). Using this list, we collected external measurement

data for all species available in museum databases and the literature. These data consisted of

head and body length (total length minus the tail), tail length, hind foot length, and ear length—

all in millimeters (mm). We also collected body weight data in grams (g). The following sources

contributed most to this database: Arctos, the Collaborative Collection Management Solution

(Arctos, 2018; 47,511 observations), VertNet, a Database of Vertebrate Specimen Records

(VertNet, 2019; 15,644 observations), the collections database of the Division of Mammals,

Smithsonian National Museum of Natural History (NMNH, 2018; 8,445 observations), iDigBio,

Integrated Digitized Biocollections (iDigBio, 2019; 6,667 observations), and the database of the

zoological collection of the Museum of Comparative Zoology, Harvard University (MCZbase,

2018; 1,113 observations). In total, data was collected from 285 different reference sources,

which are listed in Table S1 in the Supporting Information. The museum databases included data

from 58 natural history collections (see Table S1).

Our final database consists of measurement data for 81,880 observations, with the

number of observations per species ranging from 6,647 (Mus musculus) to several species with a

single observation (Table S1). In total, data was collected for 2,212 species (head and body

length: n = 2,212; tail length: n = 2,188; hind foot length: n = 2,160; ear length: n = 1,911; body

weight: n = 1,191), belonging to 490 genera (Table S2). According to the Mammal Diversity

Database (Burgin et al., 2018), the number of rodent species currently described is 2,552,

belonging to 513 genera, indicating that we sampled ~86% of the rodent species and ~95% of

their genera. Further details about the process of data collection, processing, cleanup, and quality

control can be found in Appendix S1. We used our database to calculate the species means

(Table S2) and standard deviations for each measurement. Because the length of species'

appendages is correlated to their body size, we need to size-correct each measurement. One

option is to calculate the relative length of each appendage by dividing it by body length (e.g.

Coetzee, 1970; Fooden & Albrecht, 1999; Bidau et al., 2011; Alhajeri, 2016). Appendage lengths

could alternatively be size corrected by computing the residuals of regressions of each species

125  mean appendage value (tail length, hind foot length, ear length) against the species mean value

126  of head and body length (used as an estimate of body size) (e.g., Alroy, 2019). Here, however,

127  we accounted for the relationship between appendage length and body size by including head

128  and body length as an additional predictor in all statistical models (see section 2.3 and 2.4 below)

129  (see Freckleton, 2002).

130

131  ## 2.2 | Environmental data collection

132  We extracted distributional data for all 2,212 rodent species from IUCN (2017). These data

133  consist of polygons depicting each species' known global range based on a combination of

134  empirical records, knowledge of elevational and habitat requirements, and expert assessment.

135  Although these range maps may not accurately represent the exact locations where species are

136  present, they are currently the best global assessment of species' distributions at a large

137  taxonomic scale (Schipper et al., 2008). We downloaded IUCN range maps as Environmental

138  Systems Research Institute (Esri) shapefiles from www.iucnredlist.org/resources/spatial-data-

139  download. We kept all polygon subsets, including invasive ranges, as they represent evidence of

140  the adaptation of species to local climates, whether they occur naturally or not. The IUCN

141  shapefiles (polygons) were loaded into R (R Development Core Team, 2019) and manipulated

142  therein using the following libraries: SF (Pebesma, 2018), RGDAL (Bivand et al., 2018),

143  RGEOS (Bivand & Rundel, 2018), and EXACTEXTRACTR (Baston 2020). We used the R

144  library LETSR (Vilela & Villalobos, 2015) to extract the range size of each species (in

145  kilometers squared) based on the IUCN polygons.

146          In addition, we used the RREDLIST R library (Chamberlain, 2018) to obtain a list of

147  habitats used by each species using the highest hierarchical level of habitat classification in

148  IUCN. We considered all categories of polygons (extant, extinct, introduced) as they represent

149  environmental conditions in which species are able to survive and reproduce, and hence are all

150  representative of their climatic niche. Out of 2,212 species, 1,257 had more than one habitat type

151  in the IUCN classification. In order to reduce habitat to one type only for each species, we

152  downloaded a global map of terrestrial habitats that uses the same IUCN classification (Jung et

153  al, 2020), and extracted the area of all habitat types within each species' range, and then

154  classified these 1,257 species according to the most common habitat. For the remaining 955

155  species, we kept the habitat type provided by the IUCN red list (Table S2). Several habitat types

156 are represented by a few species and their inclusion caused multivariate models to crash;

157 therefore, these analyses only included the six main habitat types represented by most species

158 (forest, savanna, shrubland, grassland, rocky areas desert).

159       Species were divided into one of four life modes which roughly correspond to

160 microhabitat use (arboreal [n=307], scansorial [n=173], subterranean [n=125], terrestrial

161 [n=1565]) (Table S2)—these data were downloaded from www.vertlife.org/data (Wilman et al.,

162 2014; Upham et al., 2020). These life modes are associated with consistent modifications in the

163 appendages that could influence conformity to Allen's rule. A total of 42 species in our dataset

164 did not have life mode data, and thus were not used in multivariate models that use these data.

165       Saltatorial (i.e., ricochetal) and a semi-saltatorial locomotory modes are associated with

166 consistent modifications to the appendages, which in turn could influence conformity to Allen's

167 rule. The literature was used to assign terrestrial species, based on morphological modifications

168 to saltation, into those that are fully saltatorial, semi-saltatorial, and those with no information on

169 saltation ability (Table S2). The first category (fully saltatorial [n=65]) includes such species as

170 jerboas and kangaroo rats that are extremely specialized for leaping and commonly employ a

171 bipedal hopping gait almost exclusively as their primary mode of locomotion. The second

172 category (semi-saltatorial [n=281]) is much less specialized for leaping (e.g., gerbils and pocket

173 mice) which often use other locomotory modes (e.g., ambulatory or cursorial locomotion), but

174 assume a (quadrupedal) jumping gait on occasion, such as when alarmed to escape predators

175 (i.e., as a secondary mode of locomotion). All other species are included in the third category (no

176 information [n=1866]), which are species for which we could not find any strong evidence in the

177 literature for specialization to saltation (see Table S2 for details).

178       Allen's rule is commonly explained in terms of the thermoregulation hypothesis, and thus

179 mainly makes predictions about appendage lengths relative to environmental temperature.

180 However, as both temperature and precipitation exhibit strong latitudinal variation, we aimed to

181 disentangle the role of several climate variables in driving the latitudinal patterns in

182 morphological variation. To test which variable contributes to explaining Allen's rule, we used

183 six bioclimatic variables depicting both average annual and maximum and minimum temperature

184 (in °C) and precipitation (in millimeters): BIO1 (annual mean temperature), BIO5 (maximum

185 temperature of the warmest month), BIO6 (minimum temperature of the coldest month), BIO12

186 (annual precipitation), BIO13 (precipitation of the wettest month), and BIO14 (precipitation of

187 the driest month) (for details, see Busby, 1991). These bioclimatic variables were downloaded as

188 raster files from WorldClim (version 2), at a resolution of 2.5 arc-min

189 (http://worldclim.org/version2, Fick & Hijmans, 2017), and processed using the R library

190 RASTER (Hijmans, 2017). Version 2 of the WorldClim dataset is based on average temperature

191 and precipitation interpolated from a global database of weather stations, spanning the years

192 1970 to 2000 (Hijmans, 2017).

193        Among rodent species, the latitudinal midpoint of geographic ranges — based on the

194 centroid of IUCN range maps — is positively correlated to annual mean temperature (Pearson's r

195 $= 0.743$, $p < 0.050$) and negatively to annual precipitation (Pearson's r = -0.633, $p < 0.050$). In

196 addition, high pairwise correlations exist among the temperature variables (Pearson's r = 0.480–

197 0.942, all $p < 0.050$) and precipitation variables (Pearson's r = 0.490–0.886, all $p < 0.050$).

198

## 2.3 | Data analysis

200 We analyzed the effect of climate on rodents' appendage length both across species and across

201 assemblages. For each type of analysis and for each appendage, we followed the same analytical

202 steps. First, we examined geographical patterns of appendage length by testing the association

203 between appendage length and the absolute value of latitude. Second, we assessed how this

204 pattern could be explained by climatic factors by testing the effect of each of the six bioclimatic

205 variables on the appendage lengths. We selected the best fitting variable among them—the one

206 that leads to the model with the lowest Akaike information criterion score, corrected for small

207 sample size (AICc; Akaike, 1974; Burnham & Anderson, 2002). In all models, we included as

208 explanatory variables both the climate variable to be tested and head and body length to control

209 for the effect of body size on appendage length. An additional null model was computed,

210 excluding climate from the explanatory variables. Third, we computed multivariate models with

211 interactions to test for the effect of various species' characteristics (body size, habitat type, range

212 size, life mode, and saltation ability) on the relationship between appendage length and the

213 selected climate variable.

214        To account for intraspecific phenotypic variability that may bias comparative analyses

215 across multiple species (Garamszegi & Møller, 2010; Silvestro et al., 2015), we repeated all

216 statistical models 100 times, each time sampling a random value of appendage length and head

217 and body length, following a truncated normal distribution (so that sampled values remain > 0)

218 with the mean and standard deviation obtained from the observed distribution of values in our

219 database of morphological measurements. Note that for species where measures originated from

220 one single individual, standard deviation = 0 and the same value was sampled at each repetition.

221 Similarly, there may exist large intraspecific variation in the environmental conditions

222 experienced by a species, especially if it is distributed across a large geographical range. To

223 account for this source of uncertainty we also sampled at each iteration, in the cross-species

224 analyses, a random value of the climate variable following a normal distribution with the mean

225 and standard deviation of the observed climate within the species' range.

226       In all analyses, climate variables, as well as each morphological measurement (tail

227 length, hind foot length, ear length), were scaled and centered to allow post-hoc comparisons of

228 effect sizes (the standardized beta slope coefficients [cross-species: $\beta_{CS}$; cross-assemblage: $\beta_{CA}$]).

229 Appendage lengths, as well as head and body lengths, were also log-transformed before scaling

230 to linearize the relationships and to reduce the influence of outliers. Plots were generated using

231 the R base library and/or the following libraries: GGPLOT2 (Wickham, 2016), PATCHWORK

232 (Pedersen, 2017), VIRIDIS (Garnier, 2018), and GGTREE (Yu et al., 2017). For all analyses, the

233 significance level (p) was set at $\alpha = 0.05$. All 'log' transformation applied in this paper are

234 natural logarithms. Unless otherwise stated, all other analyses and visualizations were carried out

235 using the R base library. Visual inspections of residual plots (residuals vs. predicted values) and

236 Q–Q (quantile-quantile) plots generally lend support to the distributional assumptions of the

237 residuals of all the linear regression models described below. The complete R script used to

238 perform the phylogenetic and spatial regression analyses can be found in Appendix S2.

239

240 ## 2.3.1 | Cross-species analysis

241 We first examined the association between appendage length and climate across species, using

242 morphological, geographical, and climatic data obtained at the species-level. From the IUCN

243 range maps, we extracted the mean and standard deviation of the latitudinal coordinates of each

244 species' range. Then, combining range maps with bioclimatic variables (raster files), we

245 extracted for each species the mean and standard deviation of each of the abovementioned six

246 bioclimatic variables across locations of its entire range (for details, see Alhajeri et al., 2015).

247       Because species are not independent and because there is evidence of phylogenetic

248 conservatism for all studied morphological traits (see Figures 1a, 2a, 3a), we used phylogenetic

249 regressions to correct for relatedness among species. For this purpose, we used a sample of 100

250 trees from Upham et al. (2019), the most complete mammalian phylogeny to date. This source

251 had two alternative forms of the phylogenetic trees: (1) 'DNA-only' trees, which only contain

252 the species for which DNA data was available; and (2) 'completed' trees, which also include

253 species missing DNA data that are imputed with birth-death branch lengths within genus- or

254 family-level taxonomic constraints (family if no congeners were sampled for DNA) (for details,

255 see Upham et al., 2019). The reason for analyzing a sample of 100 trees (for both the DNA-only

256 and completed trees) was to consider the uncertainty in phylogenetic placements and node ages.

257 A total of 98 species in our morphometric data set were not found in Upham et al.'s

258 (2019) trees (Table S3). For these species, we used taxonomic information from both IUCN

259 (2017) and the Integrated Taxonomic Information System (ITIS, 2018) to find synonyms to

260 match the species names from our dataset to those in the phylogenetic tree. We were able to find

261 synonyms for 56 species; the remaining 42 species were not found (Table S3), and thus were not

262 included in the cross-species analyses (but are included in the cross-assemblage analyses; see

263 below). As such, the cross-species analyses are based on 2,170 species for the completed sample

264 of trees and 1,466 species for the DNA-only trees.

265 We ran phylogenetic regressions with the length of each of the three appendages as

266 response variable and, as explanatory variables, either latitude or one of the six bioclimatic

267 variables, along with the head and body length always included as a covariable (to account for

268 size). Using the selected climatic variable (the one which leads to the lowest AICc), we

269 computed models where explanatory variables were the interactions between climate and: head

270 and body length, habitat type, range size, life mode, saltation ability as well as all main effects.

271 The significance of these interactions was assessed by likelihood-ratio tests comparing a model

272 with and without the interaction. The whole approach was repeated 100 times (because we use a

273 sample of 100 phylogenetic trees) for each of the completed and the DNA-only sample of trees.

274 In addition, for each tree, analyses were repeated 100 times (because we sampled 100 values of

275 morphology and climate), resulting in a total of 540,000 phylogenetic regressions computed (3

276 appendages [tail, ear, hind foot] $\times$ 2 types of phylogenies [DNA-only + completed] $\times$ 100 trees $\times$

277 100 random sampling $\times$ 9 sets of variables [latitude + null model + 6 bioclimatic variables +

278 interaction model]).

279        Phylogenetic linear regressions were computed using the R library PHYLOLM (Ho &

280    Ane, 2014), assuming a Pagel's lambda ($\lambda$) phylogenetic model (Pagel, 1999). Out of 100 trees

281    and 100 sampled values, we report for each climate variable and for the null model the mean

282    AICc weight of the corresponding model. We report the mean estimate of the slope of the

283    relationship between appendage length and climate, and the mean coefficient of interactions

284    between climate and continuous variables across 100 trees and 100 sampled values. For all the

285    above estimates, we also report 95% confidence intervals based on the distribution of these

286    coefficients across the 100 trees and 100 sampled values, as well as the proportion of

287    significantly positive or negative coefficients. Significance of interactions are reported as the

288    proportion of cases with p-value $< 0.05$. Finally, we extracted the mean estimate of the

289    relationship between appendage length and climate (i.e., the selected bioclimatic variable) for

290    each habitat type, life mode and saltation ability.

291        Phylogenetic trees were loaded into R and manipulated therein using the following

292    libraries: GEIGER (Harmon et al., 2008), TREEIO (Yu, 2019), and PHYTOOLS (Revell, 2012).

293    The latter R library was also used to estimate ancestral values of appendage lengths using a re-

294    rooting maximum-likelihood method implemented in order to visualize trait evolution within

295    rodent phylogeny.

296

297    **2.3.2 | Cross-assemblage analysis**

298    In addition to species-level analyses, we also examined variation in appendage lengths at the

299    level of rodent species assemblages—this entailed considering a summary value of the traits of

300    all rodent species that co-occur in a given location (i.e., assemblage). We define assemblages as

301    1.5-degree equal-area grid cells globally, following the best practice recommendations of

302    Hurlbert and Jetz (2007). This assemblage-based approach is commonly used to test

303    macroecological patterns (e.g., Meiri, 2011; Maestri et al., 2016; Alhajeri et al., 2019), and can

304    reveal different insights than the species-based approach, such as community assembly in the

305    former and trait evolution in the latter (Feldman & Meiri, 2014). We first converted IUCN range

306    polygons to presence-absence raster maps at 10 arc-min resolution using LETSR, and then

307    aggregated the maps to a resolution of 1.5 degrees (this also had the effect of reducing

308    computation time). A species was considered present in a grid cell if its distribution overlapped

309    any surface of it, ensuring that all 2,212 species (those in Table S2) were included, even those

310 with a distributional range smaller than the maps' resolution. Using the associated morphological

311 traits, we summarized in each grid cell the tail length, hind foot length, or ear length of all

312 species present in the grid cell, by the median as well as by both the 10th and 90th percentile

313 length of each appendage (see Alhajeri et al., 2019 for details). We chose the median to obtain a

314 general perspective on species' appendages within an assemblage, without resorting to the mean

315 that may be uninformative in case of highly skewed traits' distributions. In addition,

316 summarizing assemblages by the 10th and 90th percentile value of appendages' length was

317 necessary to be able to detect an effect of climate if selection acts mostly on species with

318 unusually long or short appendages.

319     To control for the effects of spatial autocorrelation, we performed spatial regressions with

320 eigenvector spatial filtering. In this procedure, we computed Moran's eigenvectors (Dray et al.,

321 2006) that describe the spatial configuration of the grid cells and included them as additional

322 predictors in the linear regressions. This ensures that the resulting $\beta$ estimates and associated p-

323 values for the variables of interest (here latitude or bioclimatic variables) are free from the effect

324 of spatial autocorrelation. To prevent overfitting, we selected a set of Moran's eigenvectors via

325 forward selection by permutation, according to the following criteria: all Moran's eigenvectors

326 are significant at the 0.05 level, the difference in model R² with the previous step is higher than

327 0.005, and the whole set of Moran's eigenvectors does not account for more than 95% of total

328 variation. The calculation of Moran's eigenvectors and the spatial regressions were performed

329 using the SPMORAN R library (Murakami & Griffith, 2019), and their selection was performed

330 using the ADESPATIAL R library (Dray et al, 2020). Because species richness is unequal across

331 assemblages, we included as a weight in the models the number of species in each assemblage.

332     Spatial regressions were run with either the median, 10th percentile, or 90th percentile

333 length of each of the three appendages in each grid cell (= assemblages) as the response variable;

334 while in all models, head and body length (median, 10th percentile, or 10th percentile value to

335 match the response variable) as well as the selected Moran's eigenvectors were used as

336 explanatory variables. Other used explanatory variables were, sequentially, either the average

337 latitude or climate (defined as each of the six bioclimatic variables) of each grid cell. When

338 assessing the effect of species' characteristics on the relationship between appendage length and

339 the selected climate (the one which leads to the model with the lowest AICc), we could not test

340 the effect of species-specific categorical variables such as life mode and saltation ability because

341  they could not be averaged at the scale of whole assemblages. However, we included the

342  interaction between climate and each of head and body length and range size (averaged within

343  species' assemblages). The interaction between climate and habitat type was also included using

344  the main habitat of each grid cell, based on the IUCN habitat map described above; this was

345  computed as the habitat type that covers the most area in each grid cell, while only retaining grid

346  cells with a habitat type corresponding to the six dominant types described above for the cross-

347  species analysis.

348      All analyses were repeated 100 times, corresponding to 100 sampled values of

349  morphological measurements. In total, 8,100 spatial regressions were computed (3 appendages

350  [tail, ear, hind foot] $\times$ 3 types of assemblage-level summaries [median, $10^{th}$, and $90^{th}$ percentiles]

351  $\times$ 100 random samples $\times$ 9 sets of variables [latitude + null model + 6 bioclimatic variables +

352  interaction model]). Significance of interactions were tested using analysis of variance

353  (ANOVA) based on type-III (partial) sums of squares as implemented in the CAR library (Fox &

354  Weisberg, 2019). The mean estimate of the relationship between appendage length and climate

355  for each habitat type was extracted using the EMMEANS R library (Lenth, 2020). We report for

356  each coefficient the mean and 95% confidence intervals based on the 100 repetitions, along with

357  the number of significantly positive and negative results.

358

## 3 | RESULTS

### 3.1 | Latitudinal patterns

361  Across assemblages, when appendage size was summarized by the median, we detected a clear

362  negative relationship between all appendages' length and absolute latitude, which was strongest

363  for tail length (average $\beta_{CA\ (median)} = -0.509$) and weak for hind foot length and ear length

364  (average $\beta_{CA\ (median)} = -0.197$ and $-0.140$, respectively; Figure S1; Table S4). This relationship

365  was also detected when using the $10^{th}$ percentile of appendage size, but only for hind foot length

366  and ear length. We found no evidence for any significant latitudinal pattern when considering the

367  $90^{th}$ percentile of appendage size. Across species, we observed a negative relationship between

368  latitude and tail length only (Figure S1; Table S4), although the evidence remains scarce (95%

369  confidence intervals slightly span 0 for completed trees and only ca. 60% of phylogenetic

370  regressions were significant). This relationship was also weaker than across assemblages

371  (average $\beta_{CS\ (DNA-only)} = -0.060$; average $\beta_{CS\ (completed)} = -0.056$). In all relationships between

372    appendage length and climatic variables described below, we similarly observed that the

373    standardized effect sizes of regression estimates were of smaller magnitude in cross-species than

374    cross-assemblage analyses.

375

376    ## 3.2 | Climatic patterns

377    ### 3.2.1 | Tail length

378    Both cross-assemblage and cross-species analyses found strong support for a positive

379    relationship between tail length and temperature, although the selected variable varied depending

380    on the type of analysis, from BIO6 for cross-species analyses (average $\beta_{CS\,(DNA\text{-}only)} = 0.106$;

381    average $\beta_{CS\,(completed)} = 0.103$) to BIO1 (median and $10^{th}$ percentile length; average $\beta_{CA\,(median)} =$

382    0.472; average $\beta_{CA\,(10th\,perc)} = 0.280$) and BIO5 ($90^{th}$ percentile length; average $\beta_{CA\,(90th\,perc)} =$

383    0.106) for cross-assemblage analyses (Table S5 and Figure 1c-d). In addition to these best fit

384    variables, we observed significant relationships between tail length and BIO1 for cross-species

385    analyses, and with all other temperature variables for the cross-assemblage analyses (except

386    BIO6 that was not significant when using $90^{th}$ percentile length). Moreover, there was also a

387    positive relationship between tail length and precipitation variables, especially BIO12 and BIO13

388    in the cross-species analyses. This relationship differed depending on the species' habitat type in

389    all cases (Table S6), although differences between habitats were not constant between analyses.

390    In the cross-species analyses, desert and forest species exhibited the strongest relationship

391    between tail length and BIO6, while shrubland species had the weakest relationship, even

392    negative on average (Figure 1d). In contrast, cross-assemblage analyses pointed to different

393    effects of habitat depending on the type of summary statistics we used, and no clear pattern

394    emerged. The median and the $10^{th}$ percentile of tail length, which were both mainly determined

395    by BIO1, had the lowest relationship with BIO1 in the forest habitat; the habitats with the

396    strongest relationship differed though (median: rocky areas and grassland; $10^{th}$ percentile: rocky

397    areas and desert). Using the $90^{th}$ percentile of tail length, we found that shrubland and savanna

398    exhibited a lower relationship between tail length and BIO5 than that of all other habitats (Figure

399    1e). Overall, there was no other evidence of interaction with species' traits in the cross-species

400    analyses, since no more than 58% of models showed a significant interaction with life mode or

401    saltation (Table S6). However, we note that marginal slopes indicate a clearly significantly

402    positive relationship between BIO6 and tail length in subterranean and non-saltating species,

403  while confidence intervals cross 0 in the other species' categories (Figure 1e). In the cross-

404  assemblage analyses, the effect of temperature on tail length increased in assemblages composed

405  of species with a small range and, only for the 90th percentile, in assemblages composed of

406  small-sized species (Figure 1e).

407

### 3.2.1 | Hind-foot length

409  There was no evidence of a relationship between hind-foot length and climate in the cross-

410  species analyses, as the null model generally had the lowest AICc (Table S5 and Figure 2b).

411  Cross-assemblage analyses revealed opposite trends depending on the summary statistics (Table

412  S5 and Figure 2b-c). Using the median or 10th percentile of hind-foot length, a temperature

413  variable had the best fit overall (BIO1 and BIO6 respectively), and there was generally a positive

414  relationship between hind-foot length and all bioclimatic variables, temperature and precipitation

415  included. However, temperature had no effect on the 90th percentile of assemblage-level hind-

416  foot length, but we observed a negative correlation with all precipitation variables (BIO12 had

417  the best fit on average). Although the effect of climate alone appeared similar, the effect of range

418  size had an opposite effect on the relationship between the median (positive) and 10th percentile

419  (negative) hindfoot length (Table S6 and Figure 2e). Using the 10th percentile, there was also a

420  negative interaction between BIO6 and body size, and a significant effect of habitat type (Table

421  S6) in which BIO6 and hindfoot length show a reduced relationship in savannas, shrublands, and

422  rocky areas compared to other habitats (Figure 2e).

423

### 3.2.3 | Ear length

425  Cross-species variation in ear length appeared to be associated with precipitation, as there was

426  strong support for a negative relationship between ear length and BIO14 (precipitation of the

427  driest month) (average $\beta_{CS\ (completed)} = -0.063$; average $\beta_{CS\ (DNA-only)} = -0.050$; Figure 3c; Table S5).

428  Cross-assemblage results were largely similar to those observed for hindfoot length (Table S5

429  and Figure 3): the median or 10th percentile of ear length were mostly determined by BIO1

430  (average $\beta_{CA\ (median)} = 0.195$) and BIO6 (average $\beta_{CA\ (10th\ perc)} = 0.230$) respectively, and were

431  positively related to both temperature and precipitation variables. In contrast, the 90th percentile

432  of assemblage-level ear length was better explained by precipitation (BIO14, average $\beta_{CA\ (90th\ perc)}$

433  = -0.070) and we observed a negative correlation with all precipitation variables (we note,

434  though, that there is also evidence for a positive relationship with BIO5). There was an effect of

435  habitat type in cross-assemblage analyses only (Table S6), that showed desert habitat to have the

436  lowest relationship between the 90th percentile ear length and precipitation, and the highest

437  relationship between median or the 10th percentile ear length and temperature (Figure 3e).

438

439  **4 | DISCUSSION**

440  We assembled for this study an unprecedentedly large database of rodents' morphological

441  measurements, which, coupled with up-to-date phylogenetic, climatic, and distributional data,

442  allowed us to investigate variation in appendage size in relation to climate at broader spatial

443  scale and taxonomic level than previous works (see Alroy, 2019 for a recent example). We also

444  accounted for intraspecific variation in morphology and in the climatic conditions encountered

445  across the range, which improves the robustness of our conclusions relative to those based on

446  species averages (Ives et al., 2007; Des Roches et al., 2018). At the global scale of order

447  Rodentia, we observed that Allen's rule seems to apply mostly for tails, as this is the only

448  appendage whose size exhibits relatively strong latitudinal variation and a relationship with

449  temperature in both cross-species and cross-assemblage analyses. Generally, the association

450  between appendage lengths and climate appeared to be more clearly detected among units of

451  assemblages than species. Part of this outcome could be driven by the conservative nature of

452  integrating both phylogenetic uncertainty and intra-specific trait variation in the cross-species

453  approach, the former of which is not considered in cross-assemblage analyses. Alternatively, we

454  hypothesize that stronger effect sizes in the cross-assemblage analyses could be caused by

455  geographically widespread species, which may disproportionally contribute to global

456  morphological gradients. If this were the case, cross-species analyses would provide a better

457  assessment of the true dynamics of Allen's rule; therefore, we will mostly focus our

458  interpretation on results that were consistently supported by both cross-species and cross-

459  assemblage analyses.

460  We found that tail lengths seem to increase toward the equator and with increasing

461  temperature. This result is partly in accordance with the desert rodent study of Alhajeri (2016) in

462  that relative tail length was associated with temperature variables (but not hind-foot length nor

463  ear length). Alroy (2019) also detected an increase in relative tail lengths in small mammals in

464  the tropics (and no increase in the size of hind feet or ears); however, in that study, increased tail

465 length was not associated with increasing temperature, as our analyses suggest. Furthermore, our

466 cross-species analyses suggest that the variation in tail length is driven by BIO6 (minimum

467 temperature of the coldest month) rather than BIO1 (mean annual temperature) or BIO5

468 (maximum temperature of the warmest month). This can be explained in terms of this association

469 being adaptive for heat conservation in cold environments (by having relatively shorter tails)

470 rather than heat dissipation in warmer environments (by having relatively longer tails). A similar

471 interpretation was proposed in birds, where appendage size (bill and tarsus lengths) was found to

472 be mostly associated with winter temperature (Nudds & Oswald, 2007; Danner & Greenberg,

473 2015; Friedman et al., 2017; Fan et al., 2019; Romano et al., 2020). Cold temperatures appear to

474 be a greater evolutionary constraint than warm ones.

475 We also found evidence that conformity to Allen's rule (in tail length) varies depending

476 on the habitat type—more specifically, a stronger pattern is observed in desert and forest species.

477 For the former, this may indicate that variation in tail length is driven by thermoregulatory

478 pressures. However, it has also been previously suggested (e.g., Alroy, 2019) that the increase in

479 tail lengths with decreasing latitude is caused by increased tropical arboreality. However, we did

480 not find an effect of life mode on the strength of the relationship between tail length and BIO6.

481 Moreover, the greater tail length increase in some deserts (e.g., Sahara, Arabia, central Asia,

482 western Australia, and to a lesser degree Mexico; Figure 1b) could be driven by increased

483 saltatorial ability in such habitats, where a longer tail aids in aerial balance (see Alhajeri, 2016).

484 Thus, convergence toward longer tails could have been driven by extreme selective pressures in

485 desert environments, as is the case in other morphological traits in desert rodents (Mares, 1975;

486 Kotler et al., 1994; Alhajeri et al., 2016; Alhajeri, 2016, 2018; Alhajeri & Steppan, 2018a, b).

487 We could not, however, test the effect of saltation ability at the scale of assemblages, and

488 analyses conducted across species did not show a significant interaction of this variable on the

489 relationship between tail length and temperature, although some results (see Figure 1e) may

490 point to a stronger relationship in non-saltating species, contradicting the hypothesis above.

491 For the 90$^{th}$ percentile, Allen's rule seems to more strongly apply in assemblages

492 composed of small-sized species, and weakly to assemblages of large-sized species. This could

493 be explained by the fact that a modification in tail length would have a disproportionately

494 stronger effect on the surface-area to volume ratio (and thus thermoregulation) in smaller rodent

495 species (see Introduction). The stronger effect of temperature on tail length in assemblages

496 composed of small-ranged species could be driven by the fact that these species are subjected to

497 a narrower range of environmental conditions for which to adapt.

498        In addition, we also observed that the variation of ear length (across species) could be

499 explained by a negative relationship between ear length and the precipitation variable BIO14

500 (precipitation of driest month). In birds, there is evidence of the opposite (positive) relationship

501 between appendage length and precipitation/humidity. Indeed, longer bills have been found to be

502 associated with higher humidity, a pattern that was attributed to the need of more efficient heat

503 dissipation at high humidity during summer, because humidity reduces evaporative cooling at

504 high temperature (Gardner et al., 2016). Here, a possible explanation for the tendency for ear

505 length to decrease with increasing precipitation could be that this pattern is adaptive in dry and

506 hot environments, where longer appendage sizes help heat dissipation as per the prediction of

507 Allen's rule. In addition, desert habitats had a strongly negative relationship between the 90th

508 percentile ear length and precipitation, which suggests that rodents in the driest desert habitats

509 have the longest ears. Although there is no clear prediction of the role precipitation may have in

510 driving appendage length variation in mammals, our results suggest that such a relationship

511 exists. More thorough investigations of the complex link between inter- or intra-specific

512 variation in appendage size and precipitation, such as non-linear relationships or interactions

513 with temperature, may help to more fully decipher the underlying mechanisms.

514        In conclusion, Allen's rule is observed at the global scale in rodents but can only be

515 confidently asserted for tails. The length of hind feet shows no relationship with climatic

516 variables in cross-species, phylogenetically informed analyses. The case of ear length is

517 somewhat intermediate: measured across species, it does not show latitudinal variation nor a

518 relationship with temperature, but it appeared to be associated with global variation in

519 precipitation. Furthermore, it seems that certain species characteristics either promote or hinder

520 the observance of this rule, while others have no effect upon it. Therefore, we provide evidence

521 here of a strong departure from the global expectations of Allen's rule, i.e. a general increase in

522 the length of all appendages with increasing temperature. Most likely, this pattern reflects trade-

523 offs between selection for thermoregulation and for alternative traits (locomotion, in the case of

524 tails and hind feet). Additional studies on other taxa, conducted at the same global spatial scale

525 and high taxonomic resolution, would help assess whether conformity to Allen's rule can be

526  considered a general, widespread pattern, or is a more idiosyncratic pattern restricted to a few

527  species groups and specific appendages.

528

529  **DATA ACCESSIBILITY**

530  All data and R code generated in this study are available in the supporting information.

531

532  ACKNOWLEDGMENTS -.

533  FUNDING -.

534  AUTHOR CONTRIBUTIONS -.

535

536  **REFERENCES**

537  Akaike, H. (1974) A new look at the statistical model identification. IEEE Transactions on

538      Automatic Control, 19, 716–723.

539  Alhajeri, B. H., Hunt, O. J., & Steppan, S. J. (2015). Molecular systematics of gerbils and

540      deomyines (Rodentia: Gerbillinae, Deomyinae) and a test of desert adaptation in the

541      tympanic bulla. Journal of Zoological Systematics and Evolutionary Research, 53, 312–

542      330.

543  Alhajeri, B. H. (2016). A phylogenetic test of the relationship between saltation and habitat

544      openness in gerbils (Gerbillinae, Rodentia). Mammal Research, 61, 1–11.

545  Alhajeri, B. H., & Steppan, S. J. (2016). Association between climate and body size in rodents: A

546      phylogenetic test of Bergmann's rule. Mammalian Biology, 81, 219–225.

547  Alhajeri, B. H. (2018). Craniomandibular variation in the taxonomically problematic gerbil

548      genus Gerbillus (Gerbillinae, Rodentia): Assessing the influence of climate, geography,

549      phylogeny, and size. Journal of Mammalian Evolution, 25, 261–276.

550  Alhajeri, B. H., & Steppan, S. J. (2018a). A phylogenetic test of adaptation to deserts and aridity

551      in skull and dental morphology across rodents. Journal of Mammalogy, 99, 1197–1216.

552  Alhajeri, B. H., & Steppan, S. J. (2018b). Community structure in ecological assemblages of

553      desert rodents. Biological Journal of the Linnean Society, 124, 308–318.

554  Alhajeri, B. H., & Fourcade, Y. (2019). High correlation between species-level environmental

555      data estimates extracted from IUCN expert range maps and from GBIF occurrence data.

556      Journal of Biogeography, 46, 1329–1341.

557  Alhajeri, B. H., Porto, L. M. V., & Maestri, R. (2019). Habitat productivity is a poor predictor of
558      body size in rodents. Current Zoology, zoz037. https://doi.org/10.1093/cz/zoz037

559  Allen, J. A. (1877). The influence of physical conditions in the genesis of species. Radical
560      Review, 1, 108–140.

561  Alroy, J. (2019). Small mammals have big tails in the tropics. Global Ecology and
562      Biogeography, 28, 1042–1050.

563  Arctos (2018). Arctos, Collaborative Collection Management Solution. Downloaded on 2018
564      September 18. http://arctos.database.museum

565  Ashton, K. G., Tracy, M. C., Queiroz, A. (2000). Is Bergmann's Rule Valid for Mammals? The
566      American Naturalist, 156, 390–415.

567  Daniel Baston. (2020). exactextractr : Fast Extraction from Raster Datasets using Polygons. R
568      package version 0.4.0. https://CRAN.R-project.org/package=exactextractr

569  Bergmann, C. (1847). Über die Verhältnisse der Wärmeökonomie der Thiere zu ihrer Grösse.
570      Göttinger Studien, 3, 595–708.

571  Bidau, C., Martí, D., & Medina, A. (2011). A test of Allen's rule in subterranean mammals: The
572      genus Ctenomys (Caviomorpha, Ctenomyidae). Mammalia, 75, 311–320.

573  Bivand, R., & Rundel, C. (2018). rgeos: Interface to Geometry Engine-Open Source (GEOS). R
574      package version 0.3-28. https://CRAN.R-project.org/package=rgeos

575  Bivand, R., Keitt, T., & Rowlingson, B. (2018). rgdal: Bindings for the 'Geospatial' Data
576      Abstraction Library. R package version 1.3-3. https://CRAN.R-project.org/package=rgdal

577  Blackburn, T. M., & Hawkins, B. A. (2004). Bergmann's rule and the mammal fauna of northern
578      North America. Ecography, 27, 715–724.

579  Blix, A. S., (2016). Adaptations to polar life in mammals and birds. Journal of Experimental
580      Biology, 219, 1093–1105.

581  Burgin, C. J., Colella, J. P., Kahn, P. L., & Upham, N. S. (2018). How many species of mammals
582      are there? Journal of Mammalogy, 99, 1–14.

583  Burnham, K. P., & Anderson, D. R. (2002). Model Selection and Multi-Model Inference: A
584      Practical Information-Theoretic Approach. Springer-Verlag, New-York.

585  Busby, J. R. (1991). BIOCLIM: a bioclimate analysis and prediction system. Plant Protection
586      Quarterly, 61, 8–9.

587    Chamberlain, S. (2018). rredlist: 'IUCN' Red List Client. R package version 0.5.0.

588        https://CRAN.R-project.org/package=rredlist

589    Coetzee, C. G. (1970). The Relative Tail-Length of Striped Mice Rhabdomys pumilio Sparrman

590        1784 in Relation to Climate. Zoologica Africana, 5, 1–6.

591    Danner, R. M., & Greenberg, R. (2015). A critical season approach to Allen's rule: bill size

592        declines with winter temperature in a cold temperate environment. Journal of

593        Biogeography, 42, 114–120.

594    Des Roches, S., Post, D.M., Turley, N.E., Bailey, J.K., Hendry, A.P., Kinnison, M.T.,

595        Schweitzer, J.A. & Palkovacs, E.P. (2018) The ecological importance of intraspecific

596        variation. Nature Ecology & Evolution, 2, 57–64.

597    Dray, S., Legendre, P., & Peres-Neto, P. R. (2006). Spatial modelling: a comprehensive

598        framework for principal coordinate analysis of neighbour matrices (PCNM). Ecological

599        Modelling, 196, 483–493.

600    Dray, S., Blanchet, G., Borcard, D., Guenard, G., Jombart, T., Larocque, G., Legendre, P., &

601        Wagner, H. H. (2020). adespatial: Multivariate Multiscale Spatial Analysis. R package

602        version 0.3-8. https://CRAN.R-project.org/package= adespatial

603    Fan, L., Cai, T., Xiong, Y., Song, G., & Lei, F. (2019). Bergmann's rule and Allen's rule in two

604        passerine birds in China. Avian Research, 10, 34.

605    Feldman, A., & Meiri, S. (2014). Australian Snakes Do Not Follow Bergmann's Rule.

606        Evolutionary Biology, 41, 327–335.

607    Fick, S. E., & Hijmans, R. J. (2017). Worldclim 2: New 1-km spatial resolution climate surfaces

608        for global land areas. International Journal of Climatology, 37, 4302–4315.

609    Fooden, J., & Albrecht, G. H. (1999). Tail-Length Evolution in Fascicularis-Group Macaques

610        (Cercopithecidae: Macaca). International Journal of Primatology, 20, 431–440.

611    Fox, J., & Weisberg, S. (2019). An R Companion to Applied Regression. Third edition. Thousand

612        Oaks, CA: Sage.

613    Freckleton, R.P. (2002) On the misuse of residuals in ecology: Regression of residuals vs.

614        multiple regression. Journal of Animal Ecology, 71, 542–545.

615    Friedman, N. R., Harmáčková, L., Economo, E. P., & Remeš, V. (2017). Smaller beaks for

616        colder winters: Thermoregulation drives beak size evolution in Australasian songbirds.

617        Evolution, 71, 2120–2129.

618  Garamszegi, L. Z., & Møller, A. P. (2010). Effects of sample size and intraspecific variation in
619      phylogenetic comparative studies: A meta-analytic review. Biological Reviews, 85,
620      797-805.

621  Gardner, J. L., Symonds, M. R. E., Joseph, L., Ikin, K., Stein, J., & Kruuk, L. E. B. (2016).
622      Spatial variation in avian bill size is associated with humidity in summer among Australian
623      passerines. Climate Change Responses, 3, 11.

624  Garnier, S. (2018). viridis: Default Color Maps from 'matplotlib'. R package version 0.5.1.
625      https://CRAN.R-project.org/package=viridis

626  Gohli, J., & Voje, K.L. (2016). An interspecific assessment of Bergmann's rule in 22
627      mammalian families. BMC Evolutionary Biology, 16, 1–12.

628  Griffing, J. P. (1974). Body measurements of black-tailed jackrabbits of Southeastern New
629      Mexico with implications of Allen's rule. Journal of Mammalogy, 55, 674–678.

630  Wilman, H., Belmaker, J., Simpson, J., de la Rosa, C., Rivadeneira, M. M., & Jetz, W. (2014)
631      EltonTraits 1.0: Species-level foraging attributes of the world's birds and mammals.
632      Ecology, 95, 2027.

633  Harmon, L. J., Weir, J. T., Brock, C. D., Glor, R. E., & Challenger, W. (2008). GEIGER:
634      investigating evolutionary radiations. Bioinformatics, 24, 129–131.

635  Hijmans, R. J. (2017). raster: Geographic Data Analysis and Modeling. R package version 2.2-
636      12. https://CRAN.R-project.org/package=raster

637  Ho, L. S. T., & Ane, C. (2014). A linear-time algorithm for Gaussian and non-Gaussian trait
638      evolution models. Systematic Biology, 63, 397–408.

639  Hurlbert, A. H., & Jetz, W. (2007). Species richness, hotspots, and the scale dependence of range
640      maps in ecology and conservation. Proceedings of the National Academy of Sciences, 104,
641      13384–13389.

642  iDigBio (2019). iDigBio, Integrated Digitized Biocollections. Downloaded on 2019 July 4.
643      https://www.idigbio.org/portal/search

644  ITIS (2019). Integrated Taxonomic Information System. Accessed on 2019 October 6 – 10.
645      http://www.itis.gov

646  IUCN (2017). The IUCN Red List of Threatened Species. Version 3. Downloaded on 2019 June
647      9. https://www.iucnredlist.org

648 Ives, A.R., Midford, P.E. & Garland, T.J. (2007) Within-species variation and measurement error
649     in phylogenetic comparative methods. Systematic Biology, 56, 252–270.

650 Jung, M., Dahal, P. R., Butchart, S. H. M., Donald, P. F., De Lamo, X., Lesiv, M., Kapos, V.,
651     Rondinini, C., & Visconti, P. (2020). A global map of terrestrial habitat types [Data set].
652     Zenodo. https://doi.org/10.5281/zenodo.3816946

653 Kotler, B. P., Brown, J. S., & Mitchell, W. A. (1994). The Role of Predation in Shaping the
654     Behavior, Morphology and Community Organization of Desert Rodents. Australian Journal
655     of Zoology, 42, 449–466.

656 Lenth, R. (2020). emmeans: Estimated Marginal Means, aka Least-Squares Means. R package
657     version 1.4.6. https://CRAN.R-project.org/package=emmeans

658 Lindsay, S. L. (1987). Geographic size and non-size variation in Rocky Mountain Tamiasciurus
659     hudsonicus: significance in relation to Allen's rule and vicariant biogeography. Journal of
660     Mammalogy, 68, 39–48.

661 Maestri, R., Luza, A. L., de Barros, L. D., Hartz, S. M., Ferrari, A., de Freitas, T. R. O., &
662     Duarte, L. D. S. (2016). Geographical variation of body size in sigmodontine rodents
663     depends on both environment and phylogenetic composition of communities. Journal of
664     Biogeography, 43, 1192–1202.

665 Mainwaring, M. C., & Street, S. E. (2019). Conformity to Bergmann's rule in birds depends on
666     nest design and migration. bioRxiv, 686972. https://doi.org/10.1101/686972

667 Mammal Diversity Database (2019). American Society of Mammalogists. Accessed on 2019
668     October 4. www.mammaldiversity.org

669 Mares, M. A. (1975). South American mammal zoogeography: evidence from convergent
670     evolution in desert rodents. Proceedings of the National Academy of Sciences, 72, 1702–
671     1706.

672 Mayr, E. (1956). Geographical character gradients and climatic adaptation. Evolution, 10, 105–
673     108.

674 McCollin, D., Hodgson, J., & Crockett, R. (2015). Do British birds conform to Bergmann's and
675     Allen's rules? An analysis of body size variation with latitude for four species. Bird Study,
676     62, 404–410.

677 MCZbase (2018). Museum of Comparative Zoology, Harvard University, Database of the

678     Zoological Collections. Accessed on 2018 July 10 – August 8.

679     https://mczbase.mcz.harvard.edu

680 Meiri, S. (2011). Bergmann's Rule – what's in a name? Global Ecology and Biogeography, 20,

681     203–207.

682 Murakami, D., & Griffith, D. A. (2019). Eigenvector Spatial Filtering for Large Data Sets: Fixed

683     and Random Effects Approaches. Geographical Analysis, 51, 23–49.

684 NMNH (2018). Smithsonian National Museum of Natural History, the Division of Mammals

685     Collections Database. Downloaded on 2018 October 8.

686     https://collections.nmnh.si.edu/search/mammals

687 Nowak, R. M. (1999). *Walker's Mammals of the World. 6th Edition.* Baltimore, MA: Johns

688     Hopkins University Press.

689 Nudds, R. L., & Oswald, S. A. (2007). An interspecific test of Allen's rule: Evolutionary

690     implications for endothermic species. Evolution, 61, 2839–2848.

691 Olalla-Tárraga, M. A., Bini, L. M., Diniz-Filho, J. A. F., & Rodríguez, M. A. (2010). Cross-

692     species and assemblage-based approaches to Bergmann's rule and the biogeography of

693     body size in Plethodon salamanders of eastern North America. Ecography, 33, 362–368.

694 Pagel, M. (1999). Inferring the historical patterns of biological evolution. Nature, 401, 877–884.

695 Pebesma, E. (2018). Simple Features for R: Standardized Support for Spatial Vector Data. The R

696     Journal, 10, 439–446.

697 Pedersen, T. L. (2017). patchwork: The Composer of ggplots. R package version 0.0.1.

698     https://github.com/thomasp85/patchwork

699 R Development Core Team (2019). R: A Language and Environment for Statistical Computing.

700     Vienna, Austria: R Foundation for Statistical Computing. 3.5.3. http://www.r-project.org

701 Ray, C. (1960). The application of Bergmann's and Allen's rules to the poikilotherms. Journal of

702     Morphology, 106, 85–108.

703 Revell, L. J. (2012). phytools: an R package for phylogenetic comparative biology (and other

704     things). Methods in Ecology and Evolution, 3 217–223.

705 Romano, A., Séchaud, R. & Roulin, A. (2020) Geographical variation in bill size provides

706     evidence for Allen's rule in a cosmopolitan raptor. Global Ecology and Biogeography, 29,

707     65–75.

708 Schipper, J., Chanson, J. S., Chiozza, F., Cox, N. A., Hoffmann, M., Katariya, V., … Young, B.
709      E. (2008). The status of the world's land and marine mammals: Diversity, threat, and
710      knowledge. Science, 322, 225–30.

711 Serrat, M. A., King, D. & Lovejoy, C.O. (2008) Temperature regulates limb length in
712      homeotherms by directly modulating cartilage growth. Proceedings of the National
713      Academy of Sciences, 105, 19348–19353.

714 Silvestro, D., Kostikova, A., Litsios, G., Pearman, P. B., & Salamin, N. (2015). Measurement
715      errors should always be incorporated in phylogenetic comparative analysis. Methods in
716      Ecology and Evolution, 6, 340-346.

717 Stevenson, R. D. (1986). Allen's rule in North American rabbits (Sylvilagus) and hares (Lepus) is
718      an exception, not a rule. Journal of Mammalogy, 67, 312–316.

719 Symonds, M. R. E., & Tattersall, G. J. (2010). Geographical variation in bill size across bird
720      species provides evidence for Allen's rule. The American Naturalist, 176, 188–197.

721 Tilkens, M. J., Wall-Scheffler, C., Weaver, T. D., & Steudel-Numbers, K. (2007). The effects of
722      body proportions on thermoregulation: An experimental assessment of Allen's rule. Journal
723      of Human Evolution, 53, 286–291.

724 Upham, N. S., Esselstyn, J. A., & Jetz, W. (2019). Inferring the mammal tree: Species-level sets
725      of phylogenies for questions in ecology, evolution, and conservation. PLOS Biology, 17,
726      e3000494.

727 Upham, N. S., Esselstyn, J. A., & Jetz, W. (2020) Ecological causes of uneven speciation and
728      species richness in mammals. bioRxiv, 504803.

729 VertNet (2019). VertNet, a Database of Vertebrate Specimen Records. Downloaded on 2019
730      June 29. http://portal.vertnet.org/search

731 Vilela, B., & Villalobos, F. (2015). letsR: a new R package for data handling and analysis in
732      macroecology. Methods in Ecology and Evolution, 6, 1229–1234.

733 Wickham, H. (2016). ggplot2: Elegant Graphics for Data Analysis. New York: Springer-Verlag
734      New York. http://ggplot2.org

735 Yu, G. (2019). treeio: Base Classes and Functions for Phylogenetic Tree Input and Output. R
736      package version 1.6.2. https://guangchuangyu.github.io/software/treeio

737    Yu, G., Smith, D., Zhu, H., Guan T., & Lam, T. T-Y. (2017). ggtree: an R package for

738        visualization and annotation of phylogenetic trees with their covariates and other associated

739        data. Methods in Ecology and Evolution, 8, 28–36.

Author Manuscript

740 **FIGURES**

741 **Figure 1.** Relationship between tail length and climatic variables. (a) Example of one of the 100

742 completed phylogenetic trees used in the phylogenetic regressions, with branch colors

743 corresponding to the maximum likelihood estimates of the ancestral states for tail length. (b)

744 Map of assemblage-level mean tail length (log-transformed) values shown at 10 arc-min

745 resolution (note that we aggregated to 1.5-degree grid cells for all assemblage-based analyses).

746 (c) Mean AICc weight of models including each bioclimatic variable or none (i.e. null model) (d)

747 Standardized effect sizes based on coefficient estimates $(\beta) \pm 95\%$ confidence intervals (CI) for

748 the regression between tail length and the climate variables at the level of species (left,

749 phylogenetic regressions) or assemblages (right, spatial regressions). Results shown in (e) are the

750 effect of the interaction between climate [i.e. the climate variable with the highest AICc weight

751 as shown in (c); results are thus averaged across the subset of models for which this variable was

752 selected] and two interacting continuous variables: range size and body size (top), as well as the

753 estimated marginal slope of the relationship between tail length and climate for each level of

754 three interacting factor variables: habitat type, life mode, and saltation ability (bottom). All

755 confidence intervals are drawn from the distribution of coefficient estimates across the 100

756 repetition of random sampling, and additionally across 100 phylogenetic trees for both the DNA-

757 only trees and the completed trees in which DNA-missing species were imputed. Tail length

758 across assemblages was summarized by either the median, the $10^{th}$ or the $90^{th}$ percentile value.

759 Climatic variables are defined as follows: BIO1=annual mean temperature, BIO5=maximum

760 temperature of the warmest month, BIO6=minimum temperature of the coldest month,

761 BIO12=annual precipitation, BIO13=precipitation of the wettest month, BIO14=precipitation of

762 the driest month. Results are also reported in Tables S4, S5, and S6. Silhouettes were

763 downloaded from publicdomainpictures.net.

764

765
766
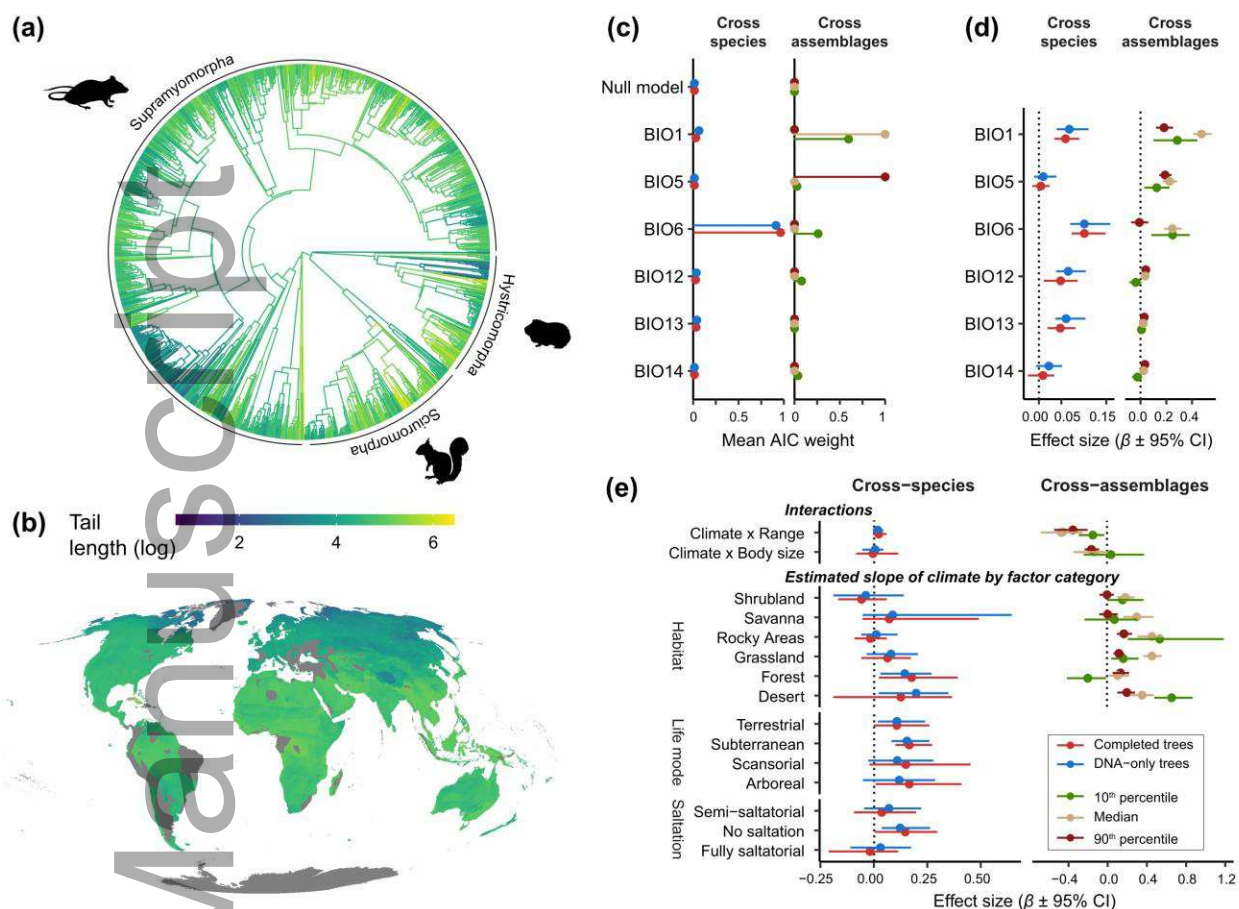
**Figure 2.** Relationship between hind foot length and climatic variables. (a) One of the 100 phylogenetic trees used in the phylogenetic regressions, with branch colors corresponding to the maximum likelihood estimates of the ancestral states for hind foot length. (b) Map of assemblage-level mean hind foot length (log-transformed) values shown at 10 arc-min resolution (assemblage-based analyses were performed in 1.5-degree grid cells). (c) Mean AICc weight of models including each bioclimatic variable or none (i.e. null model). (d) Standardized effect sizes based on coefficient estimates (ß) ± 95% confidence intervals (CI) for the regressions between hind foot length and the climate variables. (e) Interaction between the selected climate variable and species characteristics. See the Figure 1 legend for more information.

776



777
778
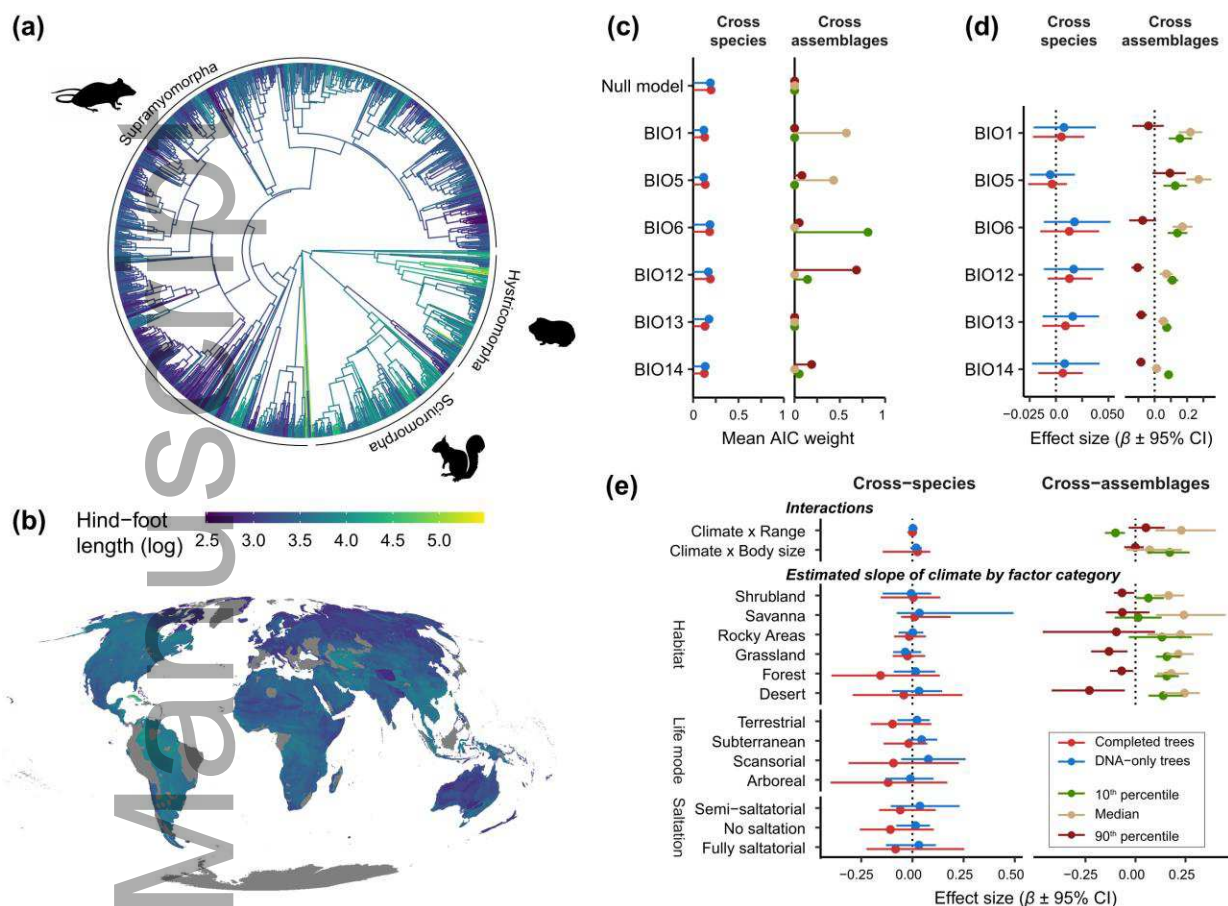
**Figure 3.** Relationship between ear length and the climatic variables. (a) One of the 100 phylogenetic trees used in the phylogenetic regressions, with branch colors corresponding to the maximum likelihood estimates of the ancestral states for ear length. (b) Map of assemblage-level mean ear length (log-transformed) values shown at 10 arc-min resolution (assemblage-based analyses were performed in 1.5-degree grid cells). (c) Mean AICc weight of models including each bioclimatic variable or none (i.e. null model). (d) Standardized effect sizes based on coefficient estimates (ß) ± 95% confidence intervals (CI) for the regressions between ear length and the climate variables. (e) Interaction between the selected climate variable and species characteristics. See the Figure 1 legend for more information.

788

789
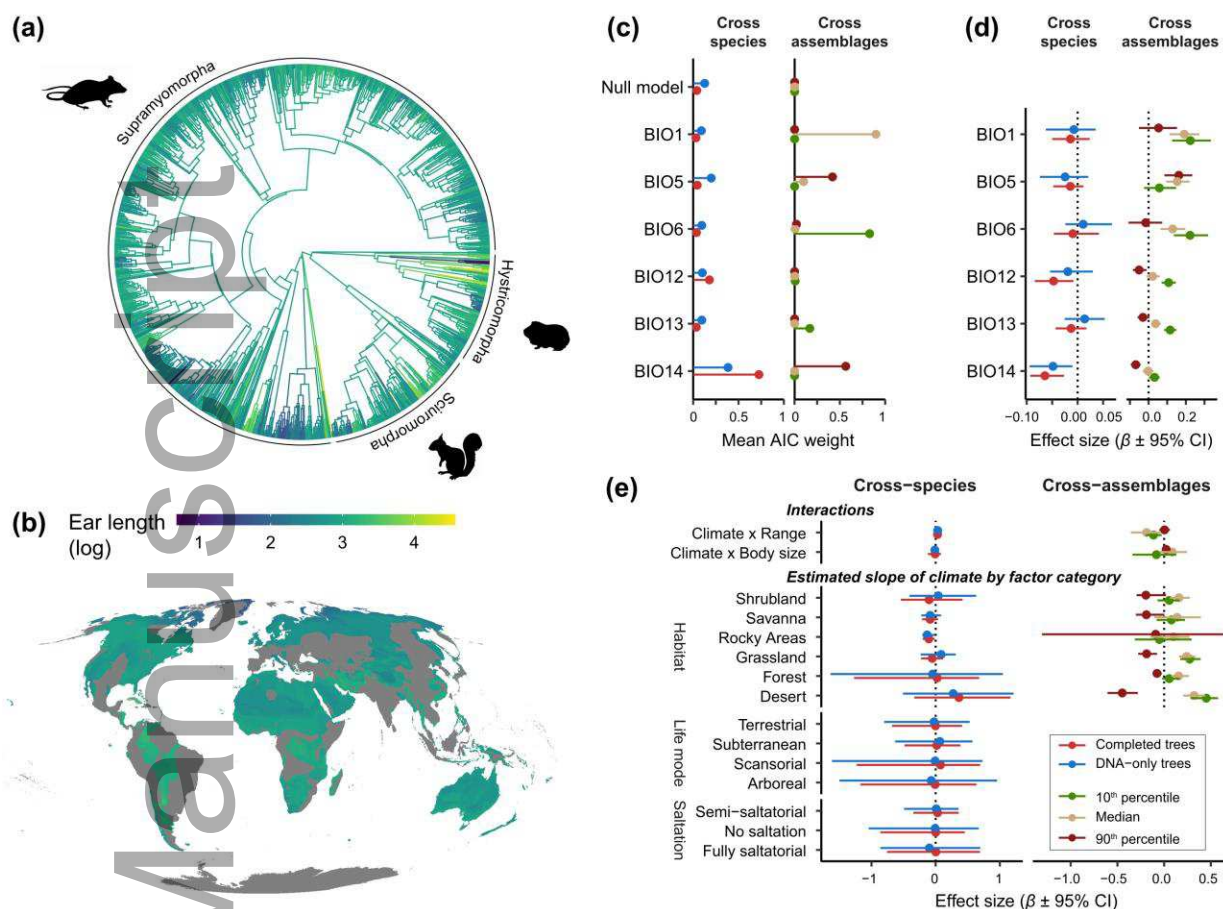
## SUPPORTING INFORMATION

**Appendix S1.** Morphometric data collection, processing, cleanup, quality control, and

preliminary analyses (supplementary methods).

**Appendix S2.** R script used to perform the phylogenetic and spatial regression analyses.

**Table S1.** Morphometric data retrieved from museum databases and the literature. The

descriptions of the columns and the abbreviations for the collections appear in the "Metadata"

sheet. The references appear in the "References" sheet. Observations (rows) lacking head and

body length and at least one appendage length (tail length, hind foot length, ear length) were not

included in this data set and thus are not used in any of the analyses. All data are untransformed.

Blank cells indicate missing data.

**Table S2.** Species means for morphometric and environmental data, along with habitat, life

mode, and saltation ability. Species means of morphometric data were calculated based on the

802    data shown in Table S1. The descriptions of the columns appear in the "Metadata" sheet. Species

803    with environmental data only (no morphometric data) were not included in this data set and thus

804    are not used in any of the analyses. All data are untransformed. Blank cells indicate missing data.
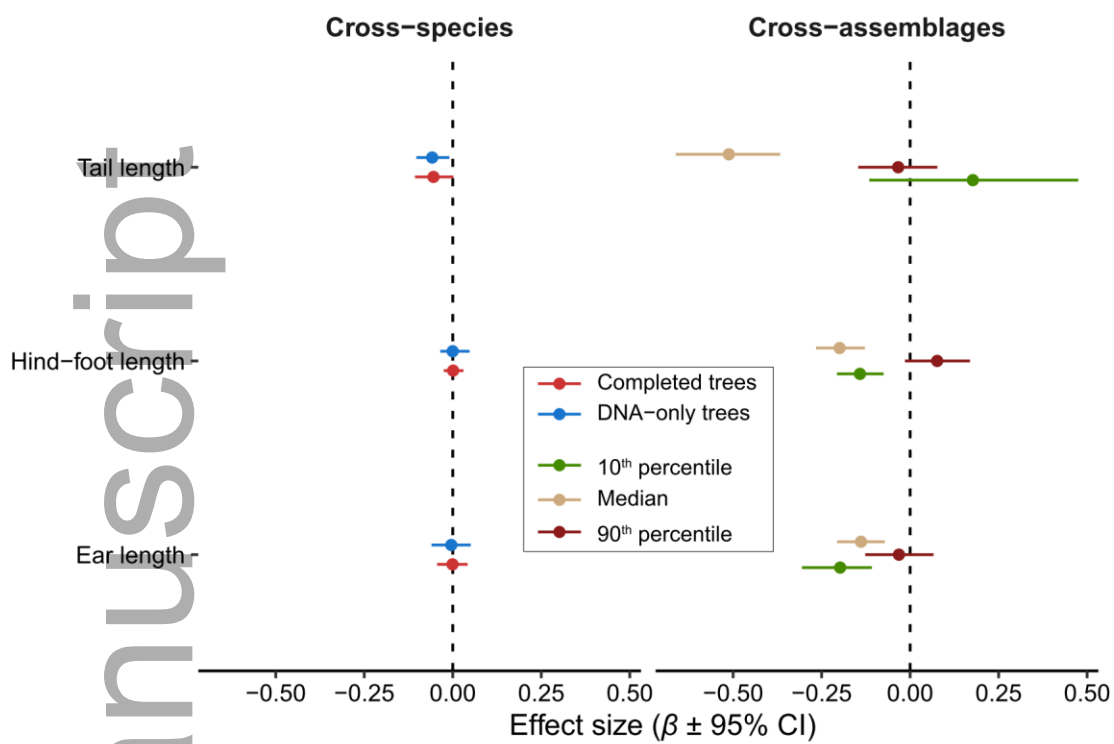
805    **Table S3.** List of species in Table S2 that are not found in the Upham et al. (2019) phylogeny,

806    and their synonyms, when available. Blank cells indicate species with no matching synonyms in

807    the Upham et al. (2019) phylogeny. See the "Metadata" sheet for more details.

808    **Table S4.** Results of the relationship between appendage length and the absolute value of

809    latitude.

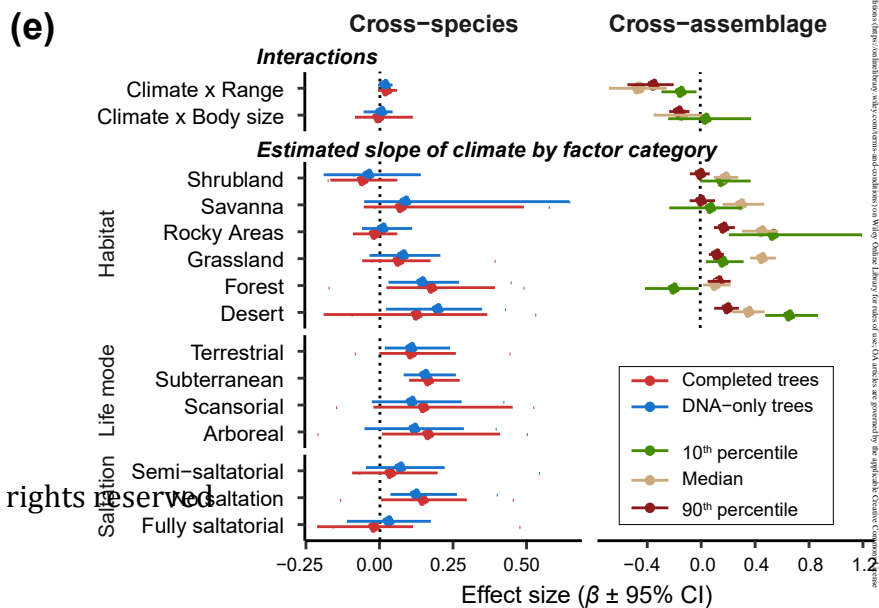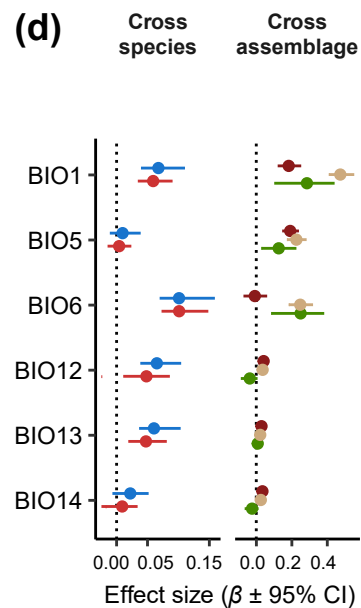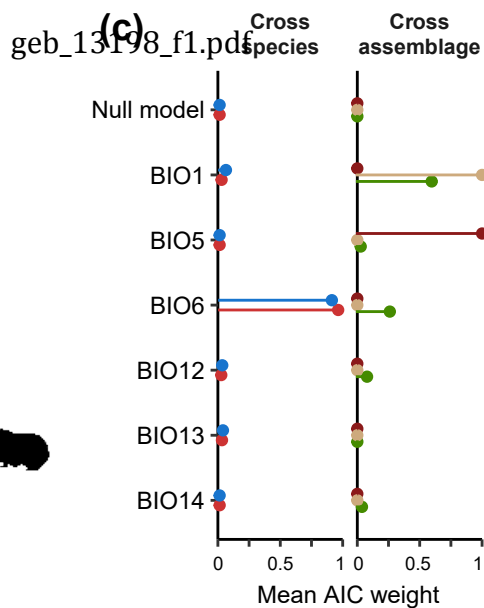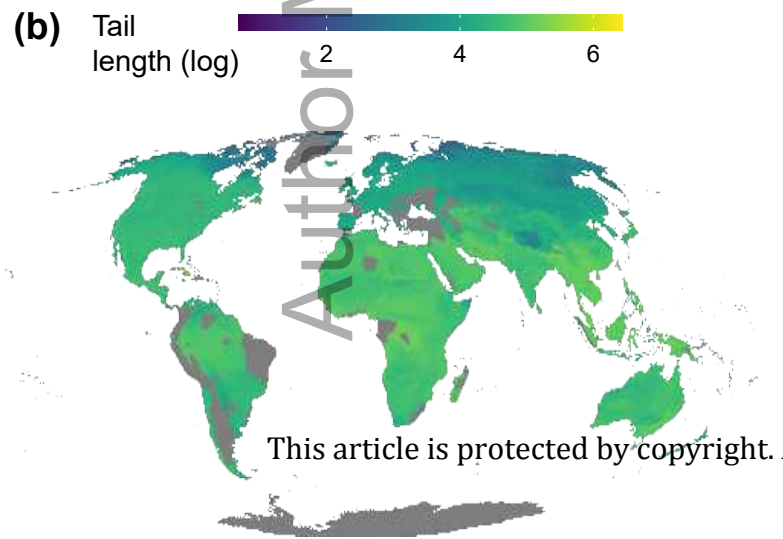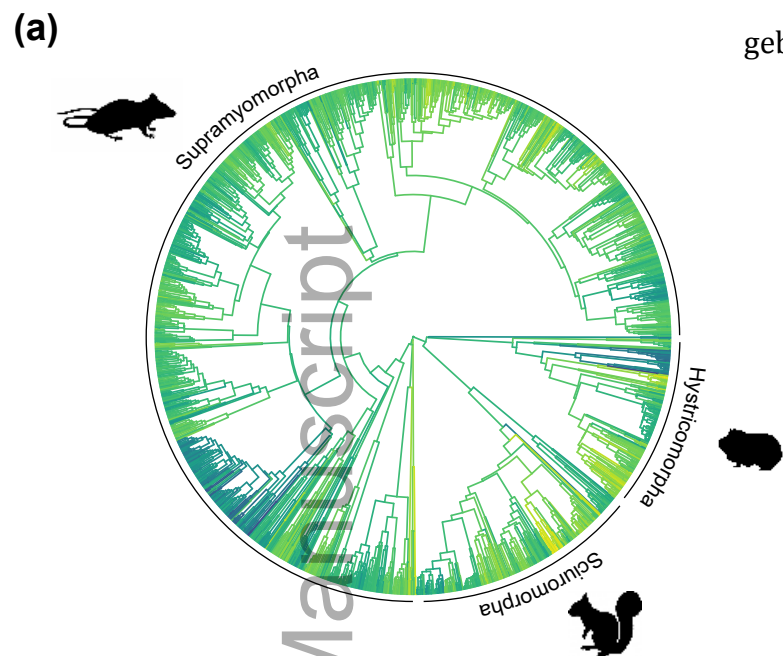810    **Table S5.** Results of the relationship between appendage length and climate.

811    **Table S6.** Proportion of significant interactions between climate and habitat, body size, range

812    size, life mode, and saltation.

813    **Figure S1.** Relationship between appendage length and latitude (absolute value). Standardized

814    effect sizes are represented as coefficient estimates (ß) ± 95% confidence intervals (CI) for the

815    regressions between tail length, hind foot length, and ear length and the absolute value of

816    latitude, for the cross-species analyses and for the cross-assemblage analyses. Results are based

817    on 100 repetitions of random sampling and, for cross-species analyses, 100 phylogenetic trees.

818    Climatic variables are defined as follows: BIO1=annual mean temperature, BIO5=maximum

819    temperature of the warmest month, BIO6=minimum temperature of the coldest month,

820    BIO12=annual precipitation, BIO13=precipitation of the wettest month, BIO14=precipitation of

821    the driest month.

822

**(a)** Supramyomorpha, Hystricomorpha, Sciuromorpha
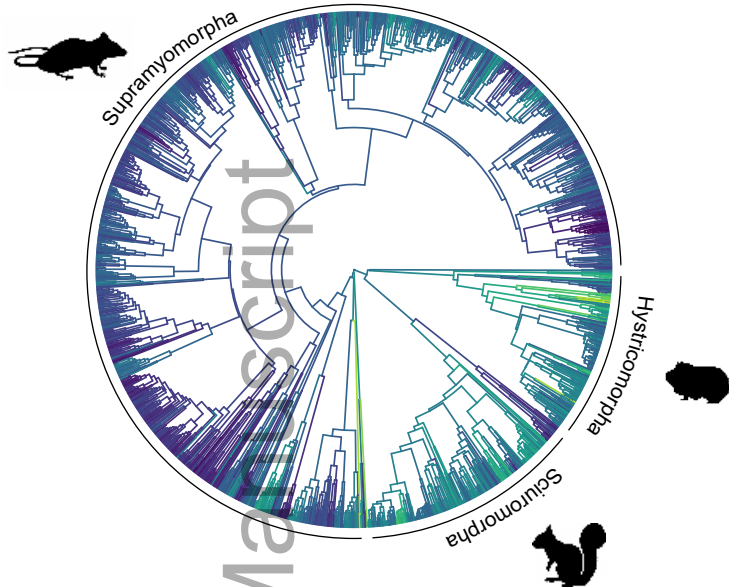
**(b)** Hind−foot length (log)
2.5  3.0  3.5  4.0  4.5  5.0

**(c)** Cross species | Cross assemblage

Null model
BIO1
BIO5
BIO6
BIO12
BIO13
BIO14

0.0  0.5  1.0  0  0.5  1
Mean AIC weight

**(d)** Cross species | Cross assemblage

BIO1
BIO5
BIO6
BIO12
BIO13
BIO14

−0.025  0.000  0.050  0.0  0.2
Effect size ($\beta \pm$ 95% CI)

**(e)** Cross-species | Cross-assemblage

*Interactions*
Climate x Range
Climate x Body size

*Estimated slope of climate by factor category*

Habitat
Shrubland
Savanna
Rocky Areas
Grassland
Forest
Desert

Life mode
Terrestrial
Subterranean
Scansorial
Arboreal

Saltation
Semi−saltatorial
Saltation
Fully saltatorial

−0.25  0.00  0.25  0.50  −0.25  0.00  0.25
Effect size ($\beta \pm$ 95% CI)

Legend:
- Completed trees
- DNA−only trees
- 10th percentile
- Median
- 90th percentile

geb_13198_f2.pdf

**(a)**

Supramyomorpha

Hystricomorpha

Sciuromorpha

**(b)** Ear length (log)

1   2   3   4

**(c)**

| | Cross species | Cross assemblage |
|---|---|---|
| Null model | | |
| BIO1 | | |
| BIO5 | | |
| BIO6 | | |
| BIO12 | | |
| BIO13 | | |
| BIO14 | | |

0   0.5   1   0   0.5   1

Mean AIC weight

**(d)**

| | Cross species | Cross assemblage |
|---|---|---|
| BIO1 | | |
| BIO5 | | |
| BIO6 | | |
| BIO12 | | |
| BIO13 | | |
| BIO14 | | |

-0.10   0.00   0.05   0.0   0.2

Effect size ($\beta \pm$ 95% CI)

**(e)**

Cross-species        Cross-assemblage

*Interactions*

Climate x Range
Climate x Body size

*Estimated slope of climate by factor category*

Habitat:
Shrubland
Savanna
Rocky Areas
Grassland
Forest
Desert

Life mode:
Terrestrial
Subterranean
Scansorial
Arboreal

Saltation:
Semi-saltatorial
Sub-saltation
Fully saltatorial

Legend:
- Completed trees (red)
- DNA-only trees (blue)
- 10th percentile (green)
- Median (tan)
- 90th percentile (dark red)

-1   0   1      -1.0   0.0   0.5

Effect size ($\beta \pm$ 95% CI)